Editor: Professor Seok Hoon Jeong

Journal Pre-proof

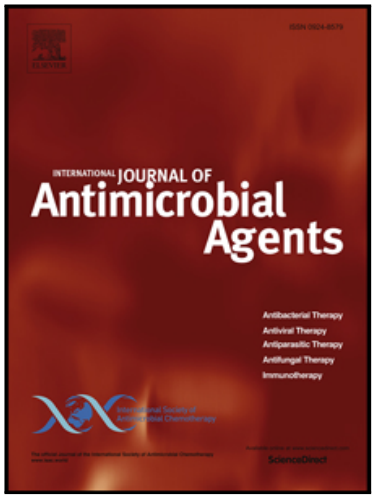

Impact of Cefiderocol on Klebsiella pneumoniae: A Population-based Longitudinal Analysis of Phenotypic and Genotypic Responses at Subinhibitory and Inhibitory Concentrations

German M. Traglia , Samyar Moheb , Usman Akhar , Cecilia Quiroga , Marisel R. Tuttobene , Mase Hamza , Fernando Pasteran , Gauri Rao , Marcelo E. Tolmasky , Robert A. Bonomo , Maria Soledad Ramirez

PII: S0924-8579(26)00133-0
DOI: https://doi.org/10.1016/j.ijantimicag.2026.107844
Reference: ANTAGE 107844

To appear in: *International Journal of Antimicrobial Agents*

Received date: 12 November 2025
Accepted date: 12 May 2026

Please cite this article as: German M. Traglia , Samyar Moheb , Usman Akhar , Cecilia Quiroga , Marisel R. Tuttobene , Mase Hamza , Fernando Pasteran , Gauri Rao , Marcelo E. Tolmasky , Robert A. Bonomo , Maria Soledad Ramirez , Impact of Cefiderocol on Klebsiella pneumoniae: A Population-based Longitudinal Analysis of Phenotypic and Genotypic Responses at Subinhibitory and Inhibitory Concentrations, *International Journal of Antimicrobial Agents* (2026), doi: https://doi.org/10.1016/j.ijantimicag.2026.107844

Highlights

- Stepwise cefiderocol exposure selected recurrent *baeS* mutations (V295G/T299P).
- Population genomics revealed de novo adaptation with convergent evolutionary paths.
- *baeS* variants emerged without transcriptional changes in the BaeSR regulon.
- Iron-uptake receptors (*cirA, fepA, iroN*) and *ompK35* were downregulated under FDC.
- *blaNDM-5*, *ompK36*, and biofilm-related genes (*mrkA, wzm, wbbM*) were upregulated.
- FDC exposure increased biofilm formation but did not alter capsule production.
- Results reveal a BaeSR-centered adaptive route to early cefiderocol resistance in *K. pneumoniae*.

Impact of Cefiderocol on *Klebsiella pneumoniae*: A Population-based Longitudinal Analysis of Phenotypic and Genotypic Responses at Subinhibitory and Inhibitory Concentrations

German M. Traglia[1#], Samyar Moheb[2#], Usman Akhar[2], Cecilia Quiroga[2, 3], Marisel R. Tuttobene[2,4], Mase Hamza[2], Fernando Pasteran[5], Gauri Rao[6], Marcelo E. Tolmasky[2], Robert A. Bonomo[7,8, 9], Maria Soledad Ramirez[2].

[1]Unidad de Genómica y Bioinformática, Departamento de Ciencias Biológicas, CENUR Litoral Norte, Universidad de la República, Montevideo, Uruguay
[2]Center for Applied Biotechnology Studies, Department of Biological Science, College of Natural Sciences and Mathematics, California State University Fullerton, 800 N State College Blvd, Fullerton, CA, USA
[3]Universidad de Buenos Aires (UBA), Consejo Nacional de Investigaciones Científicas y Técnicas (CONICET), Instituto de Investigaciones en Microbiología y Parasitología Médica (IMPaM-UBA-CONICET), Departamento de Microbiología, Parasitología e Inmunología, Facultad de Medina, Buenos Aires, Argentina.
[4]Instituto de Biología Molecular y Celular de Rosario (IBR, CONICET-UNR), Rosario, Argentina
[5]Laboratorio Nacional/Regional de Referencia en Antimicrobianos, Instituto Nacional de Enfermedades Infecciosas, ANLIS Dr. Carlos G. Malbrán, Buenos Aires, Argentina
[6]University of Southern California, Los Angeles, CA 90089, USA
[7]Research Service and GRECC, Louis Stokes Cleveland Department of Veterans Affairs Medical Center, Cleveland, OH, USA
[8]Departments of Medicine, Pharmacology, Molecular Biology and Microbiology, Biochemistry, Proteomics and Bioinformatics, Case Western Reserve University School of Medicine, Cleveland, OH, USA
[9]CWRU-Cleveland VAMC Center for Antimicrobial Resistance and Epidemiology (Case VA CARES), Cleveland, OH, USA

***Corresponding author:** María Soledad Ramírez, PhD, Professor of the Dept. Biological Science, Fullerton, CA.

Email addresses: msramirez@fullerton.edu

[#]These authors contributed equally to this work

Running Title: Cefiderocol Adaptation via BaeS in *K. pneumoniae*

Keywords: Klebsiella pneumoniae; Cefiderocol; Carbapenem-resistant Enterobacterales; NDM-5; BaeSR two-component system; experimental evolution; whole-genome sequencing; adaptive resistance

Abstract:

Background: Cefiderocol (FDC) is a siderophore cephalosporin active against carbapenem-resistant *Klebsiella pneumoniae* (CRKP), but resistance has emerged, often involving iron-uptake pathways and β-lactamases. We investigated how an NDM-producing clinical isolate adapts to FDC under stepwise selective pressure.

Methods: A ST147 *K. pneumoniae* isolate (Kp-1) carrying bla_{NDM-5} and $bla_{OXA-181}$, susceptible to FDC but resistant to other agents, was propagated in iron-depleted Mueller–Hinton broth with progressive FDC exposure. Population-based whole-genome sequencing (WGS) tracked mutation dynamics, and RT-qPCR profiled 17 genes related to FDC resistance, iron acquisition, and virulence, comparing the parental population (G0) to the first exposed generation (G1 + FDC).

Results: The mean number of mutations detected in generation G1 under FDC exposure was 24.3 ± 12.2, and in generation G2, it increased to 31.7 ± 6.4. Two nonsynonymous substitutions in *baeS* (V295G and T299P) were recurrently selected, with V295G reaching ≥ 70% frequency in independent lineages, indicating convergent evolution. RT-qPCR revealed downregulation of iron-uptake and porin genes (*iroN, cirA, fepA, kfu, ompK35*), and upregulation of *entB, ompK36*, bla_{NDM-5}, and capsule-related genes (*wzm, wbbM*); *baeS/baeR* transcript levels were unchanged. Early FDC exposure enhanced biofilm formation without significantly affecting capsule production.

Conclusions: Short-term FDC exposure reproducibly selects *baeS* variants and triggers a transcriptional program reducing siderophore-receptor entry and remodeling the outer membrane. These adaptations—together with increased bla_{NDM-5} expression and biofilm formation—contribute to reduced FDC susceptibility. The recurrent *baeS* mutations (V295G/T299P) and decreased *cirA/fepA* expression may serve as early surveillance markers of FDC adaptation in *K. pneumoniae*.

Introduction:

Antimicrobial resistance (AMR) is one of the most pressing public health challenges worldwide, driven by the ability of bacteria to evolve and adapt rapidly in response to selective pressures from antibiotic use [1,2]. Among Gram-negative pathogens, *Klebsiella pneumoniae* has emerged as a critical priority due to its capacity to acquire resistance mechanisms, including those conferring resistance to carbapenems and other β-lactam antibiotics [3,4]. This bacterium is responsible for a range of severe infections, particularly in healthcare settings, where it poses a substantial threat to immunocompromised patients.

Cefiderocol (FDC) has shown potent activity against multidrug-resistant Gram-negative bacteria, including carbapenem-resistant *K. pneumoniae* (CRKP). FDC is a siderophore cephalosporin that chelates ferric iron and exploits TonB-dependent iron transport systems to facilitate active uptake across the outer membrane, a mechanism known as the 'Trojan horse' strategy. Once in the periplasm, it binds primarily to penicillin-binding protein 3 (PBP_3), inhibits peptidoglycan synthesis, and causes bacterial cell death. This dual dependence on iron transport and cell wall synthesis is particularly relevant for understanding FDC resistance, which may arise through alterations in siderophore receptor pathways, envelope permeability, β-lactamases, and adaptive regulatory responses [5,6]. Despite its effectiveness, resistance to FDC has emerged, complicating treatment strategies and highlighting the need for deeper insights into resistance mechanisms. Reports indicate that mutations in genes related to iron uptake and efflux systems, as well as the overexpression of β-lactamase genes, may play significant roles in decreasing FDC susceptibility [6–8].

Specifically, resistance to FDC in *K. pneumoniae* has been linked to mutations affecting iron-uptake receptors such as CirA and alterations in regulatory pathways that control iron acquisition. The strain Kp-1, characterized by the presence of bla_{NDM-5} and mutations in the *cirA* gene, has emerged as a model for studying FDC resistance [9,10]. Additionally, Kp-1 exhibits enhanced expression of iron transport-related genes, a feature that may contribute to its reduced susceptibility to FDC under selective pressure [10]. Previous studies by Mezcord et al. (2024) have extensively investigated the molecular mechanisms leading to FDC resistance in *K. pneumoniae*, emphasizing the genomic variability and phenotypic expression linked to reduced susceptibility [7,9,10].

The aim of this study is to identify mutation(s) responsible for FDC resistance in *K. pneumoniae (*Kp-1) by applying a genomic population approach during progressive cefiderocol exposure,

with longitudinal WGS, transcriptomic, and phenotype studies to explain how the bacteria adapt to cefiderocol exposure.

Methods:

Bacterial Strain and Growth Conditions

A *K. pneumoniae* clinical isolate Kp-1 is ST147 clone, characterized by the presence of bla_{NDM-5} and $bla_{OXA-181}$ genes, with resistance to all antibiotics except for FDC, was used in this study [9,11] (Table S1). Frozen stocks (−80 °C in 20% glycerol) were streaked to CLED (Cystine-Lactose-Electrolyte Deficient), and a single colony was inoculated in iron-depleted cation-adjusted Mueller-Hinton broth (ID-CAMHB) at 37°C with constant agitation. All experiments were conducted in biological triplicates to ensure reproducibility.

Evolution Assays

The microbiological assays were designed to assess the development of FDC resistance over two consecutive generations (G1 and G2). Each generation was exposed to different concentrations of FDC based on the initial minimum inhibitory concentration (MIC) of the parental strain (Kp-1 G0, MIC: 0.125 µg/mL). Specifically, G1 cultures were exposed to FDC at 0.5× MIC, G2 cultures were exposed to 1× MIC (Figure 1). After each 24-hour exposure, cultures were diluted 1:100 in fresh ID-CAMHB containing the respective FDC concentration. This cycle was repeated for each generation. Control cultures were grown in the absence of FDC under identical conditions.

Population Genomic Sequencing and Bioinformatic Analysis.

Genomic DNA was extracted from FDC-exposed and control populations at each generation using the DNeasy Blood & Tissue Kit (Qiagen, Germany). DNA quality and quantity were verified by Nanodrop spectrophotometry. Whole-genome sequencing (WGS) libraries were prepared using the Illumina DNA Prep Kit (Illumina, USA) and sequenced on the Illumina NovaSeqX platform to generate paired-end reads (2 × 151 bp) (Table S2).

Reads were quality-filtered using Trimmomatic v0.39 [12] and aligned to the Kp-1 reference genome with BWA-MEM v0.7.17 [13]. Genome annotation was performed using Prokka [14]. Variant calling was performed using Breseq in polymorphism mode, followed by mutation processing with gdtools, and mutations were filtered based on minimum depth (≥10×) and quality score (≥30) [15]. Mutations were classified as synonymous or nonsynonymous.

Comparative analyses were carried out across all three biological replicates (R1, R2, R3) to identify generation-specific and shared mutations. For validation of the ancestral genomic background, pairwise comparisons of pre-exposure (G0) replicates were conducted to evaluate the baseline genetic divergence using VCFtools [16].

A maximum likelihood phylogenetic tree was constructed based on core genome SNPs using IQ-TREE v2.1.4 with 1,000 bootstrap replicates and visualized with iTOL [17,18]. We included genomes from NCBI Genomes database belonging to the same sequence type (ST) to avoid lineage bias (Table S2). These analyses confirmed that observed mutations in FDC-exposed populations arose during the experimental evolution and were not attributable to pre-existing genomic variability.

Antimicrobial Susceptibility Testing

Antimicrobial susceptibility testing was conducted to evaluate the impact of FDC exposure across successive generations of Kp-1. Minimum inhibitory concentrations (MICs) were determined using the E-Strip method in accordance with the Clinical and Laboratory Standards Institute (CLSI) guidelines [19]. The minimum inhibitory concentrations (MICs) of FDC were determined using broth microdilution (BMD) assays with iron-depleted cation-adjusted Mueller-Hinton broth (ID-CAMHB) following the Clinical and Laboratory Standards Institute (CLSI) guidelines. In addition, disk diffusion (DD) assays were performed using FDC disks (30 µg, Liofilchem S.r.l., Italy) on Mueller-Hinton agar (MHA), and the inhibition zone diameters were measured after 24 hours of incubation at 37°C. DD was to screen for resistant subpopulations, defined as colonies emerging within the zone of inhibition. CLSI and EUCAST guidelines (https://www.eucast.org/clinical_breakpoints) were used for FDC categorization using the most current breakpoints available. *E. coli* ATCC 25922 and *P. aeruginosa* ATCC 27853 served as controls.

Biofilm and Capsule Formation

Biofilm formation was assessed using the crystal violet staining method as previously described [9]. Briefly, overnight cultures of each strain were diluted to an OD600 of 0.05 and inoculated in 96-well polystyrene plates containing ID-CAMHB with or without FDC at 0.5× and 1× MIC concentrations. After 24 hours of incubation at 37°C, wells were washed with phosphate-buffered saline (PBS) and stained with 0.1% crystal violet. Excess stain was removed, and the bound dye was solubilized with 95% ethanol. Absorbance was measured at 570 nm using a microplate reader (Bio-Rad, USA).

RNA Extraction and RT-qPCR Analysis

Total RNA was extracted from G0 and G1 exposed to FDC cultures using the Direct-zol RNA Miniprep Kit (Zymo Research, USA) following the manufacturer's protocol. The RNA concentration and purity were determined spectrophotometrically. RNA samples were DNase-treated (Thermo Fisher Scientific, Waltham, MA, USA) following the manufacturer's instructions. Complementary DNA (cDNA) synthesis was performed using the iScript™ cDNA Synthesis Kit (Bio-Rad, USA).

Reverse Transcription-Quantitative PCR (RT-qPCR) was performed to assess the relative expression levels of 17 target genes, including *pbp2*, *pbp3*, *entB*, *iroN*, *cirA*, *fepA*, *ompK35*, *ompK36*, *kfu*, bla_{NDM-5}, *wzm*, *wbbM* and *mrkA*, with *rpoB* serving as the internal normalizer. The RT-qPCR reactions were carried out using the qPCRBIO SyGreen Blue Mix Lo-ROX (PCR Biosystems, USA) in a CFX96 Touch™ Real-Time PCR Detection System (Bio-Rad, USA). Relative gene expression was calculated using the 2^(-ΔΔCt) method, with statistical significance determined by two-way ANOVA followed by Tukey's post hoc test ($p < 0.05$) (Table S3).

The data obtained were statistically analyzed using GraphPad Prism (GraphPad Software, USA) to identify significant differences in gene expression and FDC susceptibility across generations.

Results:

Emergence of FDC-Resistant Variants in Kp-1 Through Evolution Assays

The microbiological assays conducted in Kp-1 involved three independent biological replicates (R1, R2, and R3), each subjected to FDC exposure across two generations (G1 and G2) (Figure 1). For each generation, the treatment groups included both FDC-exposed and control (non-exposed) conditions. The results revealed a progressive increase in FDC resistance across the exposed replicates. This phenotypic trend was supported by susceptibility testing of recovered derivatives across generations. While G0 derivatives remained susceptible to FDC (BMD: 0.5 µg/mL), recovered G1-FDC derivatives showed increased BMD MICs of 16–32 µg/mL, and G2-FDC derivatives ranged from 16 to >32 µg/mL. In the subset additionally evaluated by gradient diffusion and disk diffusion, G1.1-FDC and G2.1-FDC exhibited elevated E-test MICs (16 and 24 µg/mL, respectively), reduced inhibition zones (8 and 6 mm), and intracolony growth, supporting reduced susceptibility and population heterogeneity under FDC selection (Table S4). Notably, only FDC-treated cultures exhibited mutations, while the controls remained genetically stable.

Across all three replicates, the mean number of mutations detected in generation G1 under FDC exposure was 24.3 ± 12.2, and in generation G2, it increased to 31.7 ± 6.4. The relatively high variability observed in G1 likely reflects heterogeneity among the three independent populations during the first exposure to FDC, whereas the lower dispersion in G2 is consistent with stronger selection and partial convergence of adaptive trajectories. Similarly, the average number of non-synonymous mutations rose from 1.7 ± 0.6 in G1 to 4.7 ± 3.8 in G2, indicating an accumulation of potentially functional mutations over time (Table S4).

To ensure that the observed mutations were the result of de novo changes under FDC pressure and not pre-existing genomic differences, the ancestral populations of each biological replicate (R1, R2, and R3) were compared. Mutation comparison across the ancestral genomes revealed minimal genetic divergence, with only a handful of differences identified between R1 vs R2 and R1 vs R3 (Table S5). This low level of variation is further supported by the phylogenetic reconstruction based exclusively on genomes of the same sequence type (ST), which showed tight clustering of the ancestral replicates (Figure S1). These results confirm that the biological replicates originated from highly similar genetic backgrounds, validating the use of this experimental design to study the emergence of resistance mutations.

Among these, recurrent nonsynonymous substitutions in the gene *baeS*—V295G and T299P—were selected under exposure to FDC. In replicate G01, both variants were already present in G1‑FDC (V295G 27.9%; T299P 14.3%), and V295G rose to 87.9% by G2‑FDC. Parallel trajectories were observed across independent lineages: in G02, V295G reached 72.5% at G2‑FDC; in G03, V295G and T299P reached 74.6% and 13.9% at G2‑FDC, respectively, indicating similar genetic pathways (Figure 1; Table S6). The *baeS* gene encodes a sensor kinase that is part of the BaeSR two‑component system, previously implicated in antibiotic envelope‑stress responses. Quantitatively, in G2‑FDC the frequency of V295G averaged 78.3% (SD 8.4). Notably, within replicate G01, V295G increased from 27.9% in G1‑FDC to 87.9% in G2‑FDC, consistent with strong selection under FDC exposure. The rise of these variants, together with the increased mutation load and reduced FDC susceptibility, supports the hypothesis that BaeSR signaling contributes to adaptive resistance under siderophore‑cephalosporin pressure.

The presence of the *baeS* mutation, coupled with the increased MIC values and reduced susceptibility to FDC, suggests a potential role of this regulatory system in mediating adaptive resistance under FDC pressure.

Differential Gene Expression Associated with FDC Resistance

To further analyze adaptation to FDC, RT-qPCR was performed to quantify the transcript levels of 17 genes linked to FDC resistance and virulence across selected generations. The parental strain (G0) served as the baseline, and expression in the first-generation FDC-exposed population (G1 + FDC) was compared to G0. Genes were grouped according to their main functional category: antibiotic resistance-related genes (*pbp2, pbp3,* $bla_{NDM-5,}$ *ompK35, ompK36, baeS, baeR*) (Figure 3 A), iron acquisition genes (*entB, iroN, fepA, cirA, irp1, fyuA, kfu*; Figure 3 B), and capsule- or biofilm-associated genes (*wzm, wbbM, mrkA*; Figure 3 C).

Among the 17 genes tested, 13 showed statistically significant differences in expression levels in the FDC-exposed population compared to the ancestral strain. Upregulation was observed for bla_{NDM-5}, *ompK36*, *entB*, *wzm*, *wbbM*, and *mrkA*. Notably, *mrkA* (encoding the major structural subunit of type 3 fimbriae involved in adhesion and biofilm formation) was significantly upregulated in G1 + FDC, suggesting a potential role of enhanced fimbrial expression in the presence of FDC. This increased expression of *mrkA* was accompanied by upregulation of the capsule-associated genes *wzm* and *wbbM*, consistent with reinforcement of the polysaccharide barrier under antibiotic stress. Together, these changes, with the increase of bla_{NDM-5} and *ompK36*, indicate a coordinated modulation of β-lactam resistance and outer-membrane permeability pathways to adapt to FDC exposure.

In contrast, significant downregulation was observed for *pbp2*, *pbp3*, *ompK35*, *iroN*, *cirA*, *fepA*, and *kfu*. These results suggest suppression of pathways involved in cell wall synthesis, iron uptake, and membrane permeability in response to FDC, which may represent an adaptive strategy to reduce drug entry and metabolic dependency on iron-mediated transport systems under antibiotic pressure.

No significant differences were observed in the expression of *baeS*, *baeR*, *irp1*, and *fyuA*, despite the recurrent identification of mutations in *baeS* through genome sequencing. This suggests that while *baeS* mutations may alter signaling within the BaeSR two-component system, such changes do not directly translate into transcriptional modulation of *baeS* or *baeR* themselves. Instead, they may affect downstream regulatory targets via non-transcriptional mechanisms.

Altogether, these findings support the hypothesis that *baeS* mutations in Kp-1 may contribute to FDC resistance through non-transcriptional or species-specific regulatory mechanisms. Taken together, these results highlight that FDC resistance in Kp-1 arises from a multifaceted adaptive response that integrates altered β-lactam resistance determinants, modulation of iron uptake systems, and enhanced expression of capsule and fimbrial genes, ultimately shaping a complex resistance and virulence phenotype.

Capsule and Biofilm Formation in FDC-Exposed Generations

Biofilm formation was assessed in the ancestral Kp-1 strain (G0) and in the FDC-exposed populations (G1 + FDC and G2 + FDC) using crystal violet staining. As shown in the quantitative analysis (OD_{592}/OD_{600}), the G1 + FDC and G2 + FDC population exhibited a significantly higher biofilm biomass compared to G0 ($p < 0.05$) (Figure S2 A). This result suggests that early exposure to sub-inhibitory concentrations of FDC promotes biofilm formation in Kp-1. Such an increase may be associated with the transcriptional upregulation of *mrkA, wzm*, and *wbbM*, suggesting also that enhanced fimbrial expression together with capsule biosynthesis contribute to a strengthened surface attachment and matrix production as part of the adaptive response to FDC stress.

Capsule production was visually assessed with sedimentation assays across G0, G1, G1+FDC, G2, and G2+FDC populations (Figure S2 B). Apparent differences in capsule formation were not observed among these conditions. These phenotypic findings partially align with the transcriptomic data, where two-capsule biosynthesis–associated genes *wzm* and *wbbM* were upregulated. The lack of an evident change in sedimentation despite the upregulation of *wzm* and *wbbM* suggests that transcriptional activation alone may not be sufficient to produce a detectable capsule-associated phenotype under our experimental conditions, and may instead reflect additional layers of regulation, delayed polysaccharide remodeling, or limited sensitivity of the sedimentation assay.

Discussion:

In this study we combined microbiological assays exerting selective pressure with population genomics and targeted transcriptional profiling to dissect early routes to FDC resistance in *K. pneumoniae* Kp-1. Under stepwise FDC exposure, resistant variants emerged reproducibly across biological replicates, with higher mutational loads in G2 than G1 and an enrichment, albeit modest of nonsynonymous changes. Minimal divergence among ancestral populations and tight phylogenetic clustering indicate that the mutations detected in exposed lineages arose de novo under FDC selection rather than reflecting standing variation. Although mutations accumulated genome-wide during early FDC exposure, we interpret only recurrent changes rising across independent lineages as the strongest candidates for adaptive selection; the remaining variants may include compensatory, biofilm-associated, or hitchhiking changes that accompany early stress adaptation rather than directly mediating FDC resistance.

A central finding was the recurrent mutation in *baeS*, the sensor kinase of the BaeSR two‑component envelope‑stress system. Population sequencing resolved two nonsynonymous substitutions selected under FDC: V295G and T299P. In G1‑FDC of replicate G01, V295G and T299P were present at 27.9% and 14.3%, respectively; by G2‑FDC, V295G rose to 87.9%. Across independent lineages at G2‑FDC, V295G averaged 78.3% (SD 8.4)—72.5% in G02 and 74.6% in G03—whereas T299P was detected only in G03 at 13.9% (across‑replicate mean 4.6%, SD 8.0 when non‑detected replicates were counted as 0%). Although RT-qPCR showed that a significant change in *baeS*/*baeR* mRNA levels was not seen, mutations in sensor kinases can rewire signaling outputs without altering transcript abundance by shifting autokinase/phosphotransfer or phosphatase activity and thereby changing the phosphorylation state of BaeR.

In Enterobacterales, BaeSR regulates envelope stress responses and drug transport, including the MdtABC/AcrD efflux systems and the periplasmic chaperone Spy [20,21]. Recent work in *A. baumannii* linked *baeS* mutations to increased FDC MICs and heightened virulence via upregulation of MacAB‑TolC and other transporters [22]. Our data are consistent with a model in which *baeS* mutation shifts the regulatory set‑point of envelope responses, facilitating adaptation to FDC without necessitating changes in *baeS/baeR* expression. This interpretation is further supported by the phenotypic data obtained from recovered generation derivatives, which showed a marked increase in FDC MICs already at G1 (16–32 µg/mL) and persistent or further increased values at G2 (16 to >32 µg/mL), compared with the susceptible parental/G0 background (0.5 µg/mL). However, because population sequencing identified *baeS* substitutions within mixed evolving populations and the recovered derivatives used for susceptibility testing were not genotype-confirmed single mutants, these data establish a robust temporal association between recurrent *baeS* selection and reduced FDC susceptibility, but not direct causality for V295G or T299P individually.

The transcriptional pattern observed when comparing G0 and G1 exposed to FDC complements and supports this interpretation. Siderophore receptor genes mediating outer-membrane entry (*cirA*, *fepA*, *iroN*) and iron uptake (*kfu*) were downregulated, while *entB* (enterobactin biosynthesis) was upregulated. Given FDC's "Trojan horse" strategy, iron chelation with TonB‑dependent uptake [6], the repression of entry receptors with sustaining iron homeostasis via endogenous siderophore biosynthesis would be expected to limit FDC influx without starving the cell and allowing *K. pneumoniae* to grow. In K. pneumoniae, CirA loss/deficiency is repeatedly linked to reduced FDC susceptibility [4,9], consistent with our lower *cirA* expression. In parallel, *ompK35* decreased and *ompK36* increased, an envelope remodeling likely acting as

a secondary modifier of FDC activity, since FDC relies mainly on siderophore receptors rather than general porins for entry. Although direct regulation of *ompK36* by BaeSR has not been demonstrated here, the recurrent *baeS* mutations suggest broader envelope-stress remodeling, while the observed *ompK36* upregulation may represent a compensatory response to preserve outer-membrane homeostasis despite porin structural alterations [5,23].

A second adaptive pathway involves β‑lactamase and cell‑wall synthesis pathways. The upregulation of bla_{NDM-5} together with downregulation of *pbp2/pbp3* suggest selection for enhanced β-lactam degradation coupled to reduced peptidoglycan synthesis flux, which could blunt FDC's lethality at its periplasmic target. Although FDC is relatively stable against many β‑lactamases, elevated carbapenemase activity, including metallo‑β‑lactamases, has been associated with decreased susceptibility [4], and β‑lactamase evolution can further compromise activity [8].

Recent work by Hanna et al. (2025) reported *ybiX* mutation as part of the chromosomal background that enables high-level FDC resistance in KPC-producing *K. pneumoniae*, after experimental evolution under FDC pressure [24]. *ybiX* encodes a conserved cupin-domain protein with predicted metal-binding/periplasmic stress functions and had not previously been linked to FDC response. Notably, Hanna et al. emphasized that a single change was not sufficient; resistance emerged from combinations of β-lactamase alterations together with defects in siderophore-uptake pathways. In our evolved population, we did not detect *ybiX* mutations, reinforcing that FDC resistance is multifactorial and can arise through uncharacterized mechanisms could play a role. In our study, the recurrent *baeS* mutation, points to an alternative adaptive route centered on envelope/iron-stress signaling rather than direct inactivation of catecholate-uptake components.

Despite upregulation of capsule‑associated transcripts (*wzm, wbbM*), a visible change in capsule was not detected. However, we observed an increased biofilm formation in the strain exposed to FDC. Biofilm increase without detectable capsule changes is more consistent with regulatory remodeling than with capsule rewiring[25,26]. In *K. pneumoniae*, capsule synthesis is primarily governed by the Rcs phosphorelay; unchanged capsule metrics in our evolved populations argue against a major Rcs-driven shift [25,26]. Instead, the recurrent *baeS* mutation we observed likely tunes the BaeSR envelope-stress regulon (impacting efflux, outer-membrane permeability and adhesin display) in a way that facilitates surface attachment and matrix production while leaving capsule abundance essentially unaltered. This interpretation aligns with reports that (i) BaeS alterations can decrease FDC susceptibility via AcrD overexpression and broader envelope remodeling [5,27,28] and (ii) capsule often acts as a physical barrier to early

adhesion, so biofilm gains can arise from surface reprogramming even without capsule down-tuning [29,30].

Our data support a model in which BaeSR‑driven envelope reprogramming and iron‑uptake modulation act in cooperation with β‑lactamase upregulation to reduce FDC activity. This model aligns with prior reports implicating siderophore receptor loss (CirA), efflux and envelope‑stress regulons, and β‑lactamase activity in activity resistance across Gram‑negatives (Hong et al., 2024; Liu et al., 2023; Mezcord et al., 2024; Sato and Yamawaki, 2019) (Figure 4).

Our study has several limitations. We are aware that population WGS of short-term lineages may miss low-frequency variants and structural changes; long-read sequencing and clonal isolation will refine the mutational spectrum. In addition, although our RT-qPCR panel included *baeS/baeR* and found no differential expression, a transcriptome- and proteome-wide profiling analysis will be essential to define the BaeSR regulon in *K. pneumoniae* under FDC pressure. Lastly, functional validation (allelic repair of *baeS*, complementation) is needed to establish causality and quantify the effect on FDC MICs. However, this will be difficult to prove since, as we observed and have been observed by others [5,24,31,32], FDC resistance is multifactorial. A limitation of this study is the absence of allelic repair or complementation for *baeS*. Although such validation would strengthen causal inference, genetic manipulation in clinical multidrug-resistant *K. pneumoniae* remains technically demanding, and FDC reduced susceptibility is clearly multifactorial. We therefore interpret *baeS* as a strong candidate contributor within a broader adaptive background, and targeted mutant construction and complementation are being pursued in ongoing work.

In summary, experimental evolution of Kp-1 under cefiderocol selects for a reproducible adaptive program dominated by BaeSR‑linked envelope stress signaling, downregulation of TonB‑dependent receptors, and upregulation of $bla_{NDM‑5}$, with minimal impact on capsule and increase biofilm formation at early stages. These insights may help anticipate resistance pathways and inform surveillance markers (e.g., *baeS* variants, *cirA/fepA* expression) and therapeutic strategies that minimize selection for FDC resistance.

Data availability: All sequencing data, including FASTQ files, assembled genomes and annotations files have been deposited in Zenodo (https://zenodo.org/records/17575047)**.**

DECLARATIONS

Funding: The authors' work was supported by NIH SC3GM125556 to MSR, and 2R15 AI047115 to MET. This study was supported in part by funds and facilities provided by the

Cleveland Department of Veterans Affairs, Award Number 1I01BX001974 to RAB from the Biomedical Laboratory Research & Development Service of the VA Office of Research and Development and the Geriatric Research Education and Clinical Center VISN 10 to RAB. The content is solely the authors' responsibility and does not necessarily represent the official views of the National Institutes of Health or the Department of Veterans.

Competing Interests: The authors declare no conflict of interest.

Ethical Approval: Not required

Sequence Information: All sequencing data have been deposited in Zenodo under accession number 17575047 (https://zenodo.org/records/17575047).

Author Contributions: GMT, CQ, MRT, FP, GP, RAB and MSR conceived the study and designed the experiments. GMT, UA, SM, CQ, MRT, MH, FP, GP and MSR performed the experiments and genomics and bioinformatics analyses. GMT, CQ, MRT, FP, MET, RAB, and MSR analyzed the data and interpreted the results. FP, MET, RAB, and MSR contributed reagents/materials/analysis tools. GMT, UA, SM, CQ, MRT, MH, FP, GP, MET, RAB and MSR wrote and revised the manuscript. All authors read and approved the final manuscript.

Declaration

Given their role as an Editor for IJAA, Gauri Rao had no involvement in the peer-review of this article and has no access to information regarding its peer-review. Full responsibility for the editorial process for this article was delegated to another journal Editor”

Figure Legends

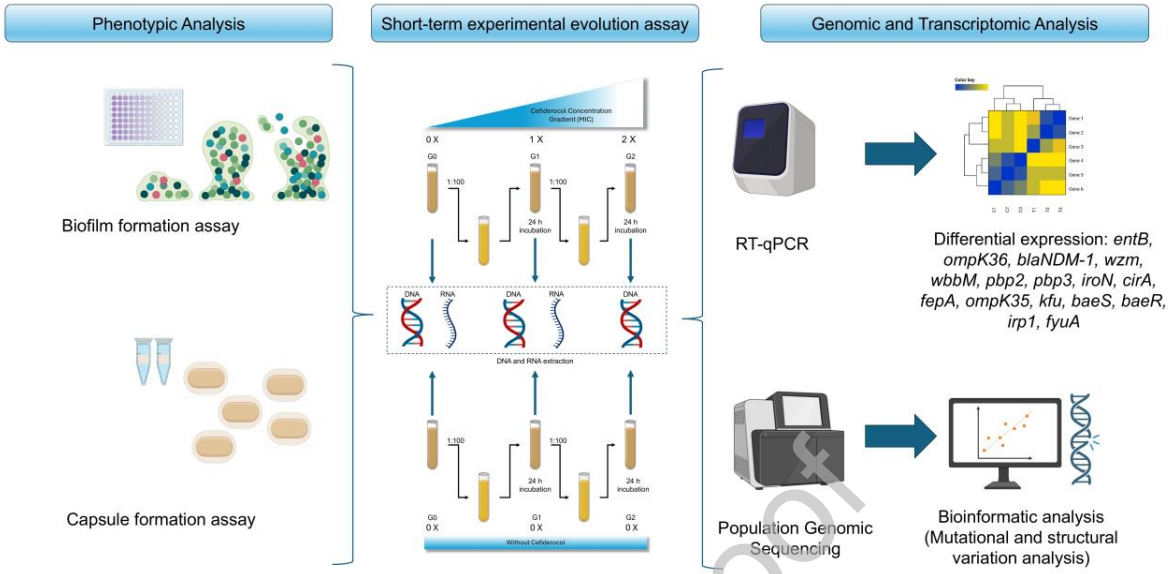

Figure 1: Experimental workflow for short-term FDC evolution and multi-level readouts. Clinical *K. pneumoniae* was passaged for 24 h cycles through a FDC concentration gradient (0×, 0.5×, 1× MIC) with 1:100 transfers between generations (G0→G1→G2); a parallel no-drug arm served as control. From each generation, DNA and RNA were extracted for population whole-genome sequencing and RT-qPCR, respectively (target genes: *entB*, *ompK36*, *bla*$_{NDM-1}$, *wzm*, *wbbM*, *pbp2*, *pbp3*, *iroN*, *cirA*, *fepA*, *ompK35*, *kfu*, *baeS*, *baeR*, *irp1*, *fyuA*). Bioinformatic analyses assessed mutational/structural variation, and phenotyping quantified biofilm and capsule formation.

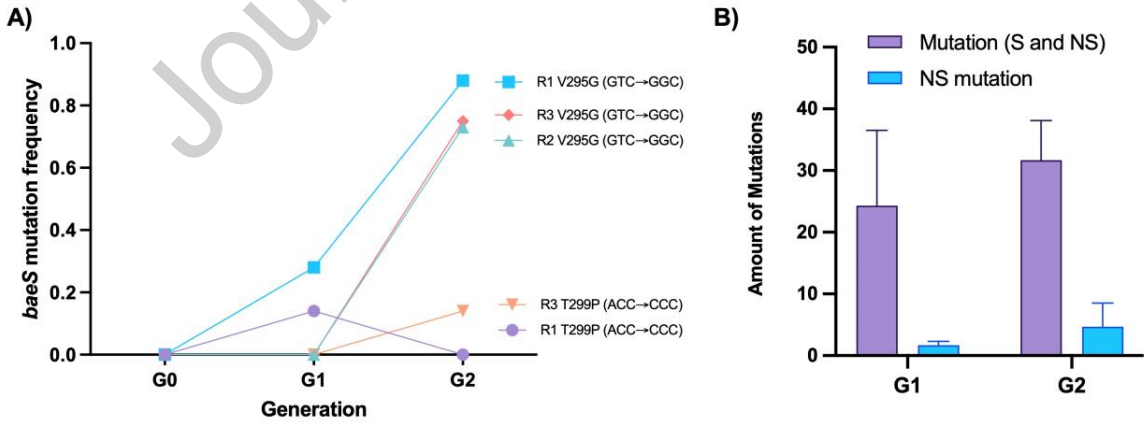

Figure 2: *baeS* mutation frequencies and genome-wide mutation load across generations. (A) Mutation frequencies of recurrent *baeS* substitutions (V295G and T299P) across generations G0–G2 in three independent lineages (R1–R3). (B) Genome-wide counts of total mutations (synonymous + nonsynonymous) and nonsynonymous (NS) mutations in G1 and G2 relative to the G0 ancestor.

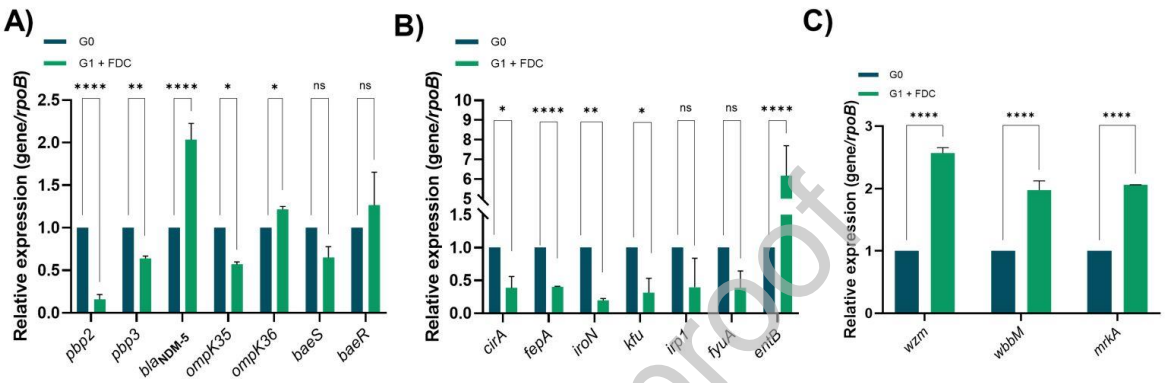

Figure 3: Expression of genes coding for antibiotic resistance-related genes (*pbp2, pbp3, bla*$_{\text{NDM-5,}}$ *ompK35, ompK36, baeS, baeR* (A), iron acquisition genes (*entB, iroN, fepA, cirA, irp1, fyuA, kfu* (B), and capsule- or biofilm-associated genes (*wzm, wbbM, mrkA* (C) in the G0 and G1 + cefiderocol strains. The data shown for qRT-PCR are mean ± SD. Fold changes were calculated using ΔΔCt analysis. At least three independent biological samples were tested using four technical replicates. Statistical significance ($p < 0.05$) was determined by two-way ANOVA followed by Tukey's multiple comparison test using GraphPad Prism Version 10.5.0 (GraphPad software, San Diego, CA, USA). Significance was indicated by: * $p < 0.05$, ** $p < 0.01$, *** $p < 0.001$, and **** $p < 0.0001$

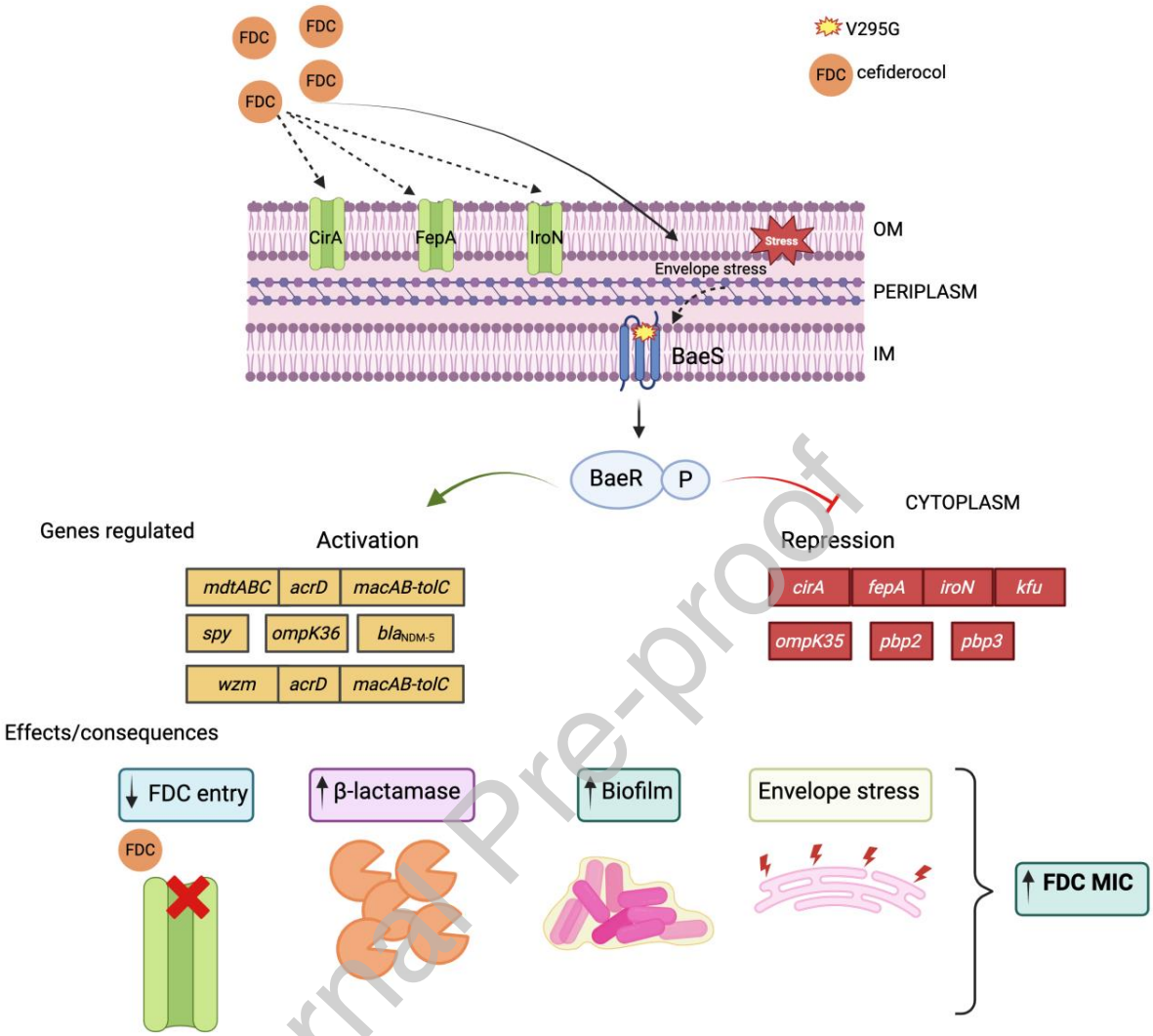

Figure 4: Model of BaeSR-mediated adaptation to cefiderocol in Kp-1. Cefiderocol (FDC) enters cells through TonB-dependent receptors (CirA, FepA, IroN). Envelope perturbation and/or altered influx are sensed by the membrane histidine kinase BaeS (mutations V295G/T299P observed under FDC selection). Altered BaeS activity changes phosphorylation of BaeR, which modulates expression of efflux pumps (e.g., *mdtABC, acrD*), periplasmic chaperones (*spy*), porins (*ompK35* ↓, *ompK36* ↑), and siderophore receptors (*cirA*, *fepA*, *iroN* ↓). These changes reduce cefiderocol influx and cooperate with upregulation of β-lactamase (blaNDM-5) and capsule/fimbrial gene expression (*wzm, wbbM, mrkA*) to increase MICs. Star on BaeS marks mutations recurrently selected (V295G mean frequency in G2 ≈ 78%).

Supplementary material

Figure S1. Core-Genome phylogeny of ancestral populations and 141 *K. pnemoniae* ST147 genomes downloaded of NCBI Genome database. The figure displays the maximum likelihood phylogeny of 144 *K. pneumoniae* genome sequences. The bootstrap method was used as a supporting method (1000 iterations). The molecular substitution model was GTR. The tree representation was done by iTOL.

Figure S2. (A) Biofilm formation in tubes quantified by crystal violet in ancestral Kp-1 strain (G0) and in the cefiderocol-exposed populations after one and two generations (G1 + FDC and G2+ FDC) strains. Statistical analysis was determined by by one-way ANOVA with post hoc testing; using Graph-Pad Prism (GraphPad software, San Diego, CA, USA); (*) indicates –values: *P < 0.05, ***P < 0.001, ****P < 0.0001. (B) Capsule density in G0, G1, G1 + FDC, G2 and G2 + FDC strains.

Table S1. MICs for Kp-1 evaluated by Etest

Table S2. List of genomes available in NCBI Genome database used in this studied (Downloaded: July 2025).

Table S3. RT-qPCR primers used in this study.

Table S4. FDC susceptibility of recovered Kp-1 derivatives from G0 to G2 assessed by broth microdilution, gradient diffusion, and disk diffusion.

Table S5. SNP and InDels prediction of evolved populations. The table lists identified mutations relative to the ancestral population (G0).

Table S6. SNP and InDels prediction among different replicates of ancestral population (G0). The table lists identified mutations comparing ancestral population: R1 vs R2; R1 vs R3 and R2 vs R3.

References:

[1] Boucher HW, Talbot GH, Bradley JS, Edwards JE, Gilbert D, Rice LB, et al. Bad bugs, no drugs: no ESKAPE! An update from the Infectious Diseases Society of America. Clin Infect Dis 2009;48:1–12. https://doi.org/10.1086/595011.

[2] Tacconelli E, Carrara E, Savoldi A, Harbarth S, Mendelson M, Monnet DL, et al. Discovery, research, and development of new antibiotics: The WHO priority list of antibiotic-

resistant bacteria and tuberculosis. Lancet Infect Dis 2017;18. https://doi.org/10.1016/S1473-3099(17)30753-3.

[3] Chen X, Sun Z, Chen J, Xu X, Wang M, Su J. The hidden threat: Klebsiella pneumoniae may develop co-resistance to colistin and cefiderocol under pressure of colistin. Int J Antimicrob Agents 2025;65. https://doi.org/10.1016/J.IJANTIMICAG.2025.107445.

[4] Hong H, Fan L, Shi W, Zhu Y, Liu P, Wei DD, et al. Overexpression of β-lactamase genes (blaKPC,blaSHV) and novel CirA deficiencies contribute to decreased cefiderocol susceptibility in carbapenem-resistant Klebsiella pneumoniae before its approval in China. Antimicrob Agents Chemother 2024;68:e0075424. https://doi.org/10.1128/AAC.00754-24/SUPPL_FILE/AAC.00754-24-S0004.DOCX.

[5] Simner PJ, Beisken S, Bergman Y, Ante M, Posch AE, Tamma PD. Defining Baseline Mechanisms of Cefiderocol Resistance in the Enterobacterales. Microb Drug Resist 2022;28:161–70. https://doi.org/10.1089/MDR.2021.0095.

[6] Sato T, Yamawaki K. Cefiderocol: Discovery, Chemistry, and In Vivo Profiles of a Novel Siderophore Cephalosporin. Clin Infect Dis 2019;69:S538–43. https://doi.org/10.1093/CID/CIZ826.

[7] Wong O, Mezcord V, Lopez C, Traglia GM, Pasteran F, Tuttobene MR, et al. Hetero-antagonism of avibactam and sulbactam with cefiderocol in carbapenem-resistant Acinetobacter spp. Microbiol Spectr 2024;12. https://doi.org/10.1128/SPECTRUM.00930-24.

[8] Findlay J, Bianco G, Boattini M, Nordmann P. High-level cefiderocol and ceftazidime/avibactam resistance in KPC-producing Klebsiella pneumoniae associated with mutations in KPC and the sensor histidine kinase EnvZ. J Antimicrob Chemother 2025;80:1155–7. https://doi.org/10.1093/JAC/DKAF048.

[9] Mezcord V, Traglia GM, Pasteran F, Escalante J, Lopez C, Wong O, et al. Characterisation of cefiderocol-resistant spontaneous mutant variants of Klebsiella pneumoniae-producing NDM-5 with a single mutation in cirA. Int J Antimicrob Agents 2024;63. https://doi.org/10.1016/J.IJANTIMICAG.2024.107131.

[10] Mezcord V, Escalante J, Nishimura B, Traglia GM, Sharma R, Vallé Q, et al. Induced Heteroresistance in Carbapenem-Resistant Acinetobacter baumannii (CRAB) via Exposure to Human Pleural Fluid (HPF) and Its Impact on Cefiderocol Susceptibility. Int J Mol Sci 2023;24. https://doi.org/10.3390/IJMS241411752.

[11] Rojas LJ, Hujer AM, Rudin SD, Wright MS, Domitrovic TN, Marshall SH, et al. NDM-5 and OXA-181 Beta-Lactamases, a Significant Threat Continues To Spread in the Americas.

Antimicrob Agents Chemother 2017;61:e00454-17. https://doi.org/10.1128/AAC.00454-17.

[12] Bolger AM, Lohse M, Usadel B. Trimmomatic: A flexible trimmer for Illumina sequence data. Bioinformatics 2014;30:2114–20. https://doi.org/10.1093/bioinformatics/btu170.

[13] Li H, Durbin R. Fast and accurate short read alignment with Burrows–Wheeler transform. Bioinformatics 2009;25:1754–60. https://doi.org/10.1093/BIOINFORMATICS/BTP324.

[14] Seemann T. Prokka: Rapid prokaryotic genome annotation. Bioinformatics 2014;30:2068–9. https://doi.org/10.1093/bioinformatics/btu153.

[15] Deatherage DE, Barrick JE. Identification of mutations in laboratory-evolved microbes from next-generation sequencing data using breseq. Methods in Molecular Biology 2014;1151:165–88. https://doi.org/10.1007/978-1-4939-0554-6_12.

[16] Danecek P, Auton A, Abecasis G, Albers CA, Banks E, DePristo MA, et al. The variant call format and VCFtools. Bioinformatics 2011;27:2156–8. https://doi.org/10.1093/BIOINFORMATICS/BTR330.

[17] Letunic I, Bork P. Interactive Tree Of Life (iTOL) v5: an online tool for phylogenetic tree display and annotation. Nucleic Acids Res 2021;49:W293–6. https://doi.org/10.1093/NAR/GKAB301.

[18] Minh BQ, Schmidt HA, Chernomor O, Schrempf D, Woodhams MD, Von Haeseler A, et al. IQ-TREE 2: New Models and Efficient Methods for Phylogenetic Inference in the Genomic Era. Mol Biol Evol 2020;37:1530–4. https://doi.org/10.1093/MOLBEV/MSAA015.

[19] CLSI M100 : performance standards for antimicrobial.35th edition 2025.

[20] Leblanc SKD, Oates CW, Raivio TL. Characterization of the induction and cellular role of the BaeSR two-component envelope stress response of Escherichia coli. J Bacteriol 2011;193:3367–75. https://doi.org/10.1128/JB.01534-10.

[21] Choudhary KS, Kleinmanns JA, Decker K, Sastry A V., Gao Y, Szubin R, et al. Elucidation of Regulatory Modes for Five Two-Component Systems in Escherichia coli Reveals Novel Relationships. MSystems 2020;5. https://doi.org/10.1128/MSYSTEMS.00980-20.

[22] Liu X, Chang Y, Xu Q, Zhang W, Huang Z, Zhang L, et al. Mutation in the two-component regulator BaeSR mediates cefiderocol resistance and enhances virulence in Acinetobacter baumannii. MSystems 2023;8. https://doi.org/10.1128/MSYSTEMS.01291-22.

[23] Wang M, Tian Y, Xu L, Zhang F, Lu H, Li M, et al. High Osmotic Stress Increases OmpK36 Expression through the Regulation of KbvR to Decrease the Antimicrobial Resistance of

Klebsiella pneumoniae. Microbiol Spectr 2022;10. https://doi.org/10.1128/spectrum.00507-22.

[24] Hanna S, La K, Yoshii Y, Gits-Muselli M, El Meouche I, Benhadid-brahmi Y, et al. Exploring mutational possibilities of KPC variants to reach high level resistance to cefiderocol. Scientific Reports 2025 15:1 2025;15:1–9. https://doi.org/10.1038/s41598-025-17044-8.

[25] Dorman MJ, Feltwell T, Goulding DA, Parkhill J, Short FL. The Capsule Regulatory Network of Klebsiella pneumoniae Defined by density-TraDISort. MBio 2018;9. https://doi.org/10.1128/MBIO.01863-18.

[26] Xu L, Li J, Wu W, Wu X, Ren J. Klebsiella pneumoniae capsular polysaccharide: Mechanism in regulation of synthesis, virulence, and pathogenicity. Virulence 2024;15. https://doi.org/10.1080/21505594.2024.2439509.

[27] Liu X, Chang Y, Xu Q, Zhang W, Huang Z, Zhang L, et al. Mutation in the two-component regulator BaeSR mediates cefiderocol resistance and enhances virulence in Acinetobacter baumannii. MSystems 2023;8. https://doi.org/10.1128/MSYSTEMS.01291-22.

[28] Nagakubo S, Nishino K, Hirata T, Yamaguchi A. The putative response regulator BaeR stimulates multidrug resistance of Escherichia coli via a novel multidrug exporter system, MdtABC. J Bacteriol 2002;184:4161–7. https://doi.org/10.1128/JB.184.15.4161-4167.2002.

[29] Sahly H, Podschun R, Oelschlaeger TA, Greiwe M, Parolis H, Hasty D, et al. Capsule impedes adhesion to and invasion of epithelial cells by Klebsiella pneumoniae. Infect Immun 2000;68:6744–9. https://doi.org/10.1128/IAI.68.12.6744-6749.2000.

[30] Nishino K, Nikaido E, Yamaguchi A. Regulation of multidrug efflux systems involved in multidrug and metal resistance of Salmonella enterica serovar Typhimurium. J Bacteriol 2007;189:9066–75. https://doi.org/10.1128/JB.01045-07.

[31] Tristancho-Baró A, López-Calleja AI, Milagro A, Ariza M, Viñeta V, Fortuño B, et al. Mechanisms of Cefiderocol Resistance in Carbapenemase-Producing Enterobacterales: Insights from Comparative Genomics. Antibiotics 2025;14:703. https://doi.org/10.3390/ANTIBIOTICS14070703/S1.

[32] Mazzitelli M, Coppi M, Scaglione V, Paci L, Castagliuolo I, Franchin E, et al. Clinical and microbiological analysis of bloodstream infections by four cefiderocol-resistant and not previously exposed NDM-producing Klebsiella pneumoniae. J Antimicrob Chemother 2025;80:2442–6. https://doi.org/10.1093/JAC/DKAF238.

Graphical_abstract